Implicit Label Number for Optical Packets in Label Switching Networks Based on Spectral Amplitude Coding and OCDM Path

Kai-Sheng Chen, *Member, IEEE*

***Abstract*—This paper presents an implicit labeling scheme where stacked spectral-amplitude-coding (SAC) labels are inscribed in multiple payload bits in the packet front. Reliable label recognition in optical packet switching (OPS) is achieved by analyzing the overall decoding results of all labeled bits instead of considering each labeled signal individually. The concept of hypothesis testing is employed to determine the optimal labeled bit number. A decision rule of correct switching is designed based on the photocurrent mean of the decoded label stacks. Considering the noise factors shown in the decoding process, the desired label number has been analyzed under different conditions of code types, label power, and the level of significance. Simulation results provide good suggestions for the tradeoff between the system insensitivity to noise effects and the transmission redundancy of carrying repetitive label information in an optical packet.**

***Index Terms*—Hypothesis testing, label stacking, optical packet switching (OPS), spectral amplitude coding (SAC).**

I. Introduction

GENERALIZED multiprotocol label switching (GMPLS) is a primary protocol for realizing optical packet switching (OPS), as it provides high efficiency in switching and bandwidth utilization with a simplified control plane [1], [2]. A packet in GMPLS is routed along a label switch path (LSP), which is established by pairs of routers reading the packet label. Packet switching can be performed by label processing executing in the time, wavelength, and space domains. Although all-optical networking is achieved, the minimum label resource in the above scenarios is restricted to an optical wavelength. If the required labels are more than the wavelengths, it may result in a reduced network capacity.

To exploit the bandwidth of a single wavelength efficiently and flexibly, GMPLS based on optical code-division multiplexing (OCDM) is proposed [3]–[5]. OCDM was originally designated for multi-user transmissions and detections in the physical layer [6], [7], and it is recently adopted as a packet-switching method in the network and data link layers [8]–[10]. Optical paths are identified by processing labels expressed as optical codes, and fine granularity is reached as multiple codes share a common wavelength resource. There are two approaches to implement a coded label in a received packet, according to the encoding part of the packet structure [11]. One is known as explicit labeling, where an OCDM signal is used as a header while the packet data is not encoded. The other is known as implicit labeling, where the label is included in all data bits by modulating each of them with a specific code sequence. The latter approach is preferred due to the simplified node architecture and efficient bandwidth utilization.

Label stacking is proposed to release the burden and simplify the structure of the forwarding nodes in core networks [12]–[14] in a code-switched GMPLS network. Rather than performing both recognition and swapping, the recognition function is sufficient for packet forwarding at each node. For packet switching based on the label codes, label stacking is realized by attaching multiple codes to a single packet. Sufficient flexibility in the network is achieved as the label number in a stack can be adjusted to fit the optical path number. Since two or more coded labels simultaneously occupy a common bandwidth, multiple access interference (MAI) is the main factor degrading the performance of label recognition. Spectral amplitude coding (SAC) has great compatibility with label stacking due to its insensitivity to the MAI effect [15], [16]. Other advantages are the low-cost codec of label generation and identification, and fast processing speed.

This paper proposes a new implicit labeling scheme where only a part of payload bits in the packet front is encoded with stacked SAC signals. It reduces the complexity of edge routers as the payload recognition can be performed by using a common photo-detector instead of a specific decoder. Since all payload bits are not necessary to carry the repetitive label information, the transmission and power efficiencies are improved. While some significant GMPLS architectures based on OCDM have been proposed in [4], [9], and [10], one of the key features of the investigated labeling scheme is that OCDM labels are generated in SAC format. SAC labels are encoded on the optical spectrum, so the chip rate equals the relatively low payload bit rate. The codec of time-spreading OCDM labels presented in the references mentioned above must be operated at a high chip rate faster several times than the bit rate. Moreover, as label stacking is employed, the packet carries the same labels throughout the entire traveling along an LSP. Each node performs label recognition for path determination. A simplified hardware architecture

Manuscript received 10 February 2022; revised 23 May 2022; accepted 27 June 2022. Date of publication 4 July 2022; date of current version 15 July 2022. This work was supported by Guangzhou Municipal Science and Technology Bureau under Grant 202002030464.

The author is with the School of Electrical and Computer Engineering, Nanfang College, Guangzhou, Guangdong 510970, China (e-mail: chenksh@nfu.edu.cn).

Digital Object Identifier 10.1109/JPHOT.2022.3188164

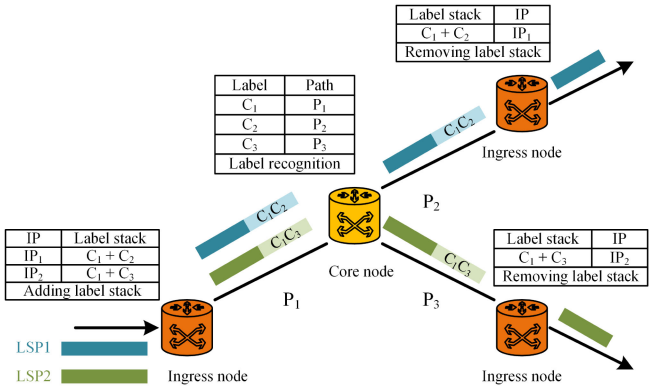

Fig. 1. GMPLS network with the label stacking of optical codes.

is achieved as only decoders are deployed in the node structure. All-optical switching can be realized as the packets stay in the optical domain during the whole switching process.

On the other hand, in other existing network architectures, the carrying labels for a packet are varied as it passes through the links between different nodes. The previous OCDM labels are removed at each node, and then the new ones are attached to the switched packet. Therefore, implementing complete sets of codecs in the node architecture becomes necessary.

However, when SAC labels are decoded, the presented noises may cause the wrong decoding results. Therefore, sufficient implicit labels are still needed to guarantee that the final decoding conclusion is correct despite some existing cases of incorrect decoding. To derive the optimal label number, we employ the concept of test statistics to analyze a Gaussian distributed model that considers the decoded photo-current of SAC labels and noise variances. The reliable label recognition in OPS can be achieved by analyzing the overall decoding results of all labeled bits instead of considering each labeled signal individually. Given an acceptable level of significance, the optimal number of labeled bits in a packet is derived for different conditions of stacked label numbers and the types of code sequences.

II. Optical Packet Switching Based on the Label Stacking of SAC Signals

Fig. 1 shows the investigated GMPLS network based on the label stacking of optical codes. We assume that the destinations of two LSPs in this network are denoted as IP_1 and IP_2. In the ingress node, the IP addresses are converted to forwarding equivalence classes (FECs) with the label stacks mapped to the LSPs. The forwarding service in the core node involves recognizing the label stack. For example, the core node executes the recognition function on the blue packet's labels and obtains the decoding results of C_1 and C_2. The path corresponding to C_2, namely P_2, is determined as the output switched path as P_1 is the input path. Please note that the stacked labels multiplexed in the same bandwidth reach a node in parallel. OCDM technique is employed to avoid interferences by allocating a specific code to each label. Only the matched label has a relatively high decoded peak, while the unmatched ones have nearly zero power at the decoder outputs.

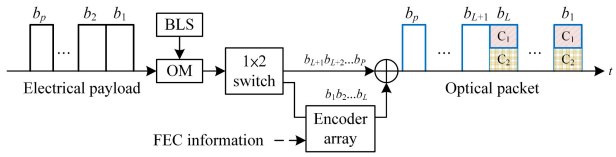

Fig. 2. The proposed packet labeling scheme with OCDM signals. BLS: broadband light source; OM: optical modulator.

In the egress node, the packet finishes its switching process. After removing the label stack, the optical payload can be recovered by conventional photo-detecting methods. As the routing algorithm is centralized to the ingress nodes, the burden and the processing speed of the core routers are incredibly released. Fast switching in the network can be achieved since label swapping/renewing in each core code is not required.

The similarity between the proposed scheme of multi-label stacking and the multi-level signaling scheme in [10] is that repetitive SAC signals are spread over the duration of a transmission unit, such as the packet frame in this paper and the bit frame. However, the proposed system is not affected by the side effect of the increased bandwidth since the label rate is fixed to the bit rate. Multiplexing gain can be obtained from increasing the labeled bit number.

Fig. 2 shows the labeling schemes of OCDM signals with label stacking. We assume that there are p payload bits in an electrical packet. In GMPLS, packets are transmitted in the optical form, so an optical modulator (OM) converts the electrical data to the optical carrier generated from a broadband light source (BLS). In this scheme, the labeling approach known as the OCDM path [11] is employed, where the labels are implicit in the payload bits. The advantage is that inserting labels does not increase the packet length or require extra bandwidth. Unlike the conventional OCDM-path method, where all p payload bits are modulated with label codes, only L out of p bits are assigned with a label stack. The L value should be properly chosen. If L is too small, the core node may not perform successful label recognition, as the correct results still cannot be obtained after the decoders have processed all labeled bits. On the other hand, a too large L results in a complicated packet structure and a reduced power efficiency. When label codes are generated, the input optical bits suffer from splitting loss when passing through the encoders. The FEC command selects the desired encoders from the encoder array to generate the stacked labels corresponding to the assigned packet path.

To support multiple traffic of optical payloads of different packets. The fiber bandwidth is divided into several wavelength channels to achieve wavelength-division multiplexing (WDM). Each channel is assigned with a packet's payload encoded with a specific label stack for switching. Since occupying different channels, multiple packets can be multiplexed without interfering with each other. Previous literature has shown that SAC is compatible with the existing WDM structure in the applications of access [17], sensor [18], and packet-switching [19] networks. Compared with the pure OCDM structure, the code-word used in the label sequence over a hybrid WDM/OCDM requires further modification.

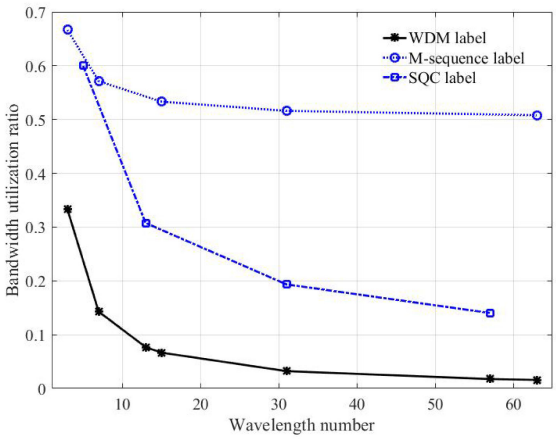

Fig. 3. Bandwidth utilization ratio versus wavelength number for WDM and OCDM labels.

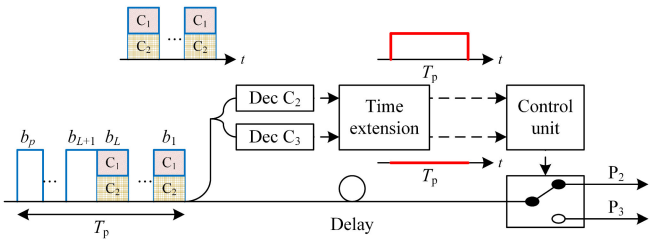

Fig. 4. Packet switching in the core node by label stack processing.

For simplicity, the proposed scheme considers multiplexing OCDM labels on a single band, while the concept can be extended to a hybrid OCDM/WDM structure with arbitrary wavelength numbers. The hybrid scheme increases flow granularity by seamlessly combining code with wavelength dimension to construct a larger label space. For a SAC label, the chips "1" and "0" in a code sequence are respectively represented by the presence and absence of a specific wavelength. Due to the good multiplexing property, SAC labels achieve more efficient bandwidth utilization than their WDM counterparts. For a channel with N wavelengths, the bandwidth utilization ratio for a single WDM label is $1/N$, while the value increases to ω/N for SAC, where ω is the code weight. As shown in Fig. 3, as N increases, the utilization ratio for a WDM label decreases, while the ratio for a SAC label reaches a nearly constant value. Code sequences of stuffed quadratic congruence (SQC) and M-sequence are selected as the two SAC labels in this figure.

Fig. 4 depicts the packet switching based on label stacking in the core node. A part of the labeled bits is extracted and then sent to decoders. The remaining packet enters a fiber delay line to wait for the decision results of label recognition. The incoming label stack is divided into copies as many as the decoder number. Then each decoder performs a correlation calculation between the label stack and the designated code. If a decoder finds a matching code in the stack, an autocorrelation signal with relatively high amplitude shows at the output. If there are no matching labels, the decoding results are a low-level cross-correlation signal. The control system connects the packet to the desired path according to the correlation values seen as the label switching information. As the time durations of the labels and a payload bit are the same, the length of the decoded signals is extended to the packet duration. Therefore, the switch keeps in a close state long enough to pass through a whole packet.

Since each pair of ingress/egress nodes in the optical network has executed routing protocol in advance, the main task of core nodes is to purely pass packets to the following nodes without analyzing the whole network condition. The switching process is based on the label distribution protocol (LDP), where the links between nodes are mapped into the optical code labels. Once an LSP is established, the ingress node configures the encoders to generate the label stack connecting with that path. When the core nodes process the optical packets, the packet labels remain the same. As label swapping is not required, the burden and system complexity in the node design is released.

Since the core nodes only run the functions in the data plane, the control planes at the ingress nodes can be easily merged into a single controller. Therefore, the packet-switching scheme can be adapted to a portion of transport software-defined networking (T-SDN) architecture. The control plane talks to the data plane via southbound commands. Once the controller identifies the route, the information of the corresponding OCDM labels and the switching table is sent to the core nodes in the data plan. The number of labeled bits is informed as well according to the required quality-of-service (QoS) determined by the controller.

Although the proposed OCDM labeling is currently implemented in OPS, its application in elastic optical network (EON) is a promising approach [20]. EON has featuring characteristics such as the adaptation to bandwidth requirements and proper resource assignment for signal routing. Similar to WDM, the number of SAC labels is determined by the sliced wavelength number in an optical band. If the label demand for a connection is low, it induces inefficient utilization of spectral resources due to the unused labels. In EON, one can compress or expand bandwidth according to the connection requirements. An expanded spectrum can be assigned to support the SAC sequences with a longer code length or a large cardinality if the required label number increases. Moreover, bandwidth-variable wavelength cross-connects (WXCs) deployed in EON could be adopted for SAC label processing, where wavelength aggregating and splitting functionalities are required.

III. Performance Analysis

A. Optimal Labeled Bit Number Derivation

The concept of hypothesis testing is adopted for determining the optimal number of the OCDM-labeled bits in an optical packet. The purpose of research hypotheses is to choose the basis for decision-making from two conflicting hypotheses about the possible values of specific matrix parameters. The scopes of the two hypotheses are mutually exclusive. When one is true, the other is false. A temporary hypothesis made for the matrix parameters is called the null hypothesis H_0, which denotes the argument to be verified. The hypothesis completely opposite to H_0 is called the alternative hypothesis H_1. In this paper, the investigated population is the decoded signals of the stacked

OCDM labels. For a packet labeled with C_i, decoder C_j, the mean of the output photocurrent μ_0 is expressed as

$$\mu_0 = \begin{cases} \frac{RP_{sr}\omega}{N}, & C_i = C_j \\ 0, & C_i \neq C_j \end{cases} \quad (1)$$

where P_{sr} is the effective light source power, and R is the photodiode responsivity. In practical scenarios, due to the noise presence, photocurrent I is a Gaussian distributed random variable denoted as $N(\mu_0,\sigma^2)$ [21], where σ^2 is also known as the noise power or the variance of I. The photocurrent variance σ^2 of the decoded SAC labels, contributed by thermal noise and phase-induced intensity noise, is expressed as

$$\sigma^2 = \left(\frac{RP_{sr}\omega}{N}\right)^2 \left(\frac{Bk}{v}\right) \left[\frac{\omega + (k-2)\,\lambda}{\omega - \lambda}\right] + BS_{th} \quad (2)$$

where λ is the label code's cross-correlation, k is the stacked label number, B is the electrical noise-equivalent bandwidth, v is the line width of the light source, and S_{th} is the power spectral density of thermal noise.

In the proposed scheme, the labels are inscribed in a portion of payload bits, and the corresponding decoding results are seen as the samples. In the previous decoding process, when $I > \mu_0/2$, the decision of $C_i = C_j$ has been made[6]. However, instead of making the decision immediately after recognizing the first labeled bit, one can obtain a more correct and adequate result of label identification until all sample information is collected. For decision making, the used parameter is the sample mean m of the decoding photocurrents of the labeled bit signals. Assuming that the label code and the decoder are matching, the definitions of the two hypotheses are expressed as

$$H_0 : \mu \geq \frac{\mu_0}{2}$$
$$H_1 : \mu < \frac{\mu_0}{2} \quad (3)$$

If H_0 is accepted during the hypothesis testing process, the label-identification result is correct. It indicates that the core node switches the packet to the correct direction regardless of the noise effects. However, if H_1 is accepted while H_0 is rejected, an incorrect result is obtained due to significant errors contributed by the noises. A packet is missed as the core node fails to orient it to the desired path. Therefore, when the hypothesis testing is performed, μ is not expected to be below $\mu_0/2$, where H_0 is rejected and the H_1 is accepted. This test is called the left-tail test since the region of accepting H_1 only appears on the left side, as shown in Fig. 5. The critical point, defined as $\mu_0/2$ in this research case, is the decision point to determine whether H_0 is accepted or rejected.

We employ the z-value test method to conduct the hypothesis testing. First, the sample mean μ is normalized to test statistic z, which expressed as

$$z = \frac{\mu - \mu_0}{\sigma/\sqrt{L}} \quad (4)$$

Second, we formulate the decision rule. As the investigated case is left-tail, the desired result is that z falls in the acceptance region of H_0. Therefore, H_0 is accepted if $z \geqq z_\alpha$, where z_α is normalized critical value determined by significance level α. Finally, the minimum number of labeled bits in a packet is expressed as

$$L \geq \left(\frac{2z_\alpha\sigma}{\mu_0}\right)^2 \quad (5)$$

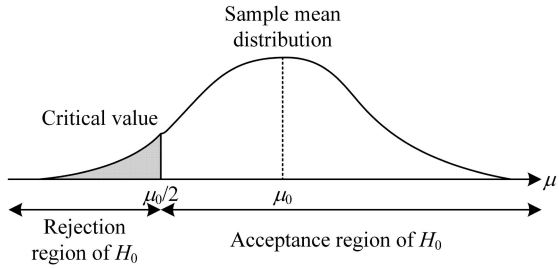

Fig. 5. The acceptance/rejection region of H_0 for the decoding photocurrent of SAC labels.

B. Bit Error Rate (BER) Evaluation

For the investigated OCDM labels of SAC, multiple-access interference (MAI) can be eliminated due to the pseudo orthogonal property among optical codes. The label information of code C_i can be identified from the multiplexed label stack without MAI by the following calculation known as correlation subtraction, which is expressed as

$$C_i \odot C_j - \frac{\lambda}{(\omega - \lambda)} C_i \odot \overline{C}_j = \begin{cases} \omega, i = j \\ 0, i \neq j \end{cases} \quad (6)$$

where $0 \leq i,j \leq N$. The symbol of $\odot$ denotes the dot-production operation.

Since the proposed OCDM scheme aims to detect packet labels efficiently, it does not influence the payload's bit error rate (BER) performance. A decoder known as balanced detector performing (6) is employed to identify all-optical codes in the label stack for label detection. On the other hand, bit detection can be achieved by employing a single photo detector. A payload bit "1" or "0" can be simply determined by the intensity of a bit pulse without knowing all its carrying labels. As MAI has a neglected effect, the primary factor influencing BER is the noise raising in the photo-detection process. Assuming that all bits "1" are transmitted in a payload, BER can be derived from the Gaussian approximation of the noise distribution, which is expressed as

$$\text{BER} = \frac{1}{2}\text{erfc}\left(\frac{\mu_b}{4\sigma_b}\right) \quad (7)$$

where μ_b and σ_b are the mean and standard deviation of the photocurrent of an optically labeled bit. According to the assumptions on the light source and deduction method in [21], μ_b and σ_b are expressed as

$$\mu_b = \frac{kRP_{sr}\omega}{N} \quad (8)$$

$$\sigma_b = \sqrt{\frac{R^2P_{sr}^2Bk}{Nv}\left[\omega + (k-1)\,\lambda\right] + BS_{th}} \quad (9)$$

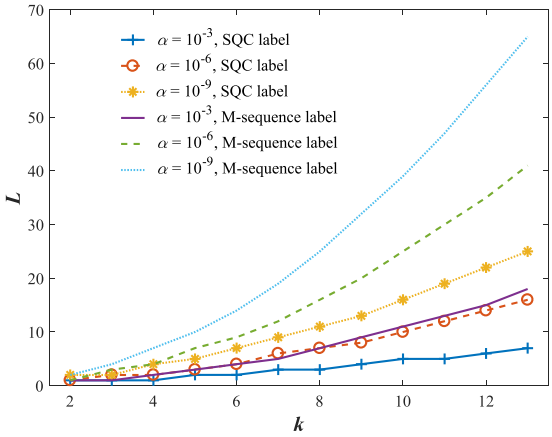

Fig. 6. L versus k for SQC and M-sequence labels.

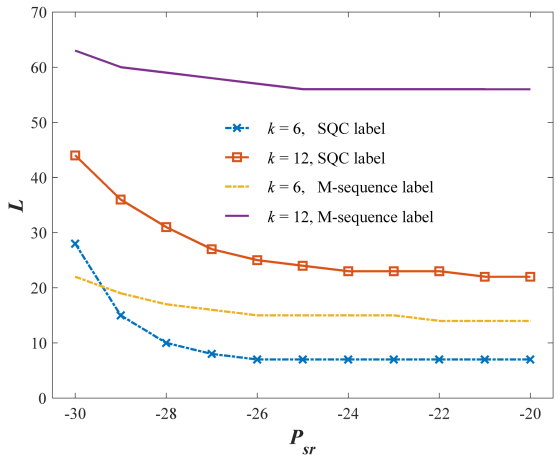

Fig. 7. L versus P_{sr} when $\alpha = 10^{-9}$.

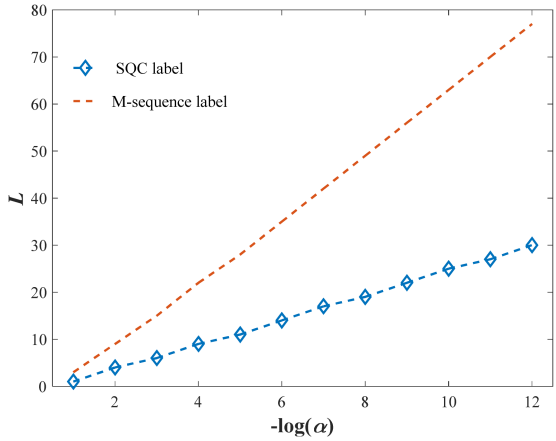

Fig. 8. L versus the level of significance α when $k = 12$.

C. Blocking Probability (BP) Evaluation

In order to analyze blocking probability (BP), the traffic behaviors at the edges of a LSP are modeled for a given load. It is assumed that the rate γ of packets arriving at the start of an LSP follows a Poisson process, and the existing time u in a path follows an exponential process. Each link is assigned with k available labels for the arrived connection requests. If all k labels are occupied, the new arrival is rejected, and packet blocking occurs. The whole process of a packet traveling along an LSP is similar to the one of entering Erlang's model of *M*/*M*//*k*/*k*. The steady-state probability of an LSP connection occupying x labels is expressed as [22]

$$P(x) = \frac{P_0}{x!}\left(\frac{\gamma}{u}\right)^x, 0 \le x \le k \tag{10}$$

The term P_0 deducted from the normalization condition is expressed as

$$P_0 = \left[\sum_{x=0}^{k} \frac{1}{x!}\left(\frac{\gamma}{u}\right)^x\right]^{-1} \tag{11}$$

Based on the above discussion, when the existing packets occupy all labels in a switching path, the connection set up asked by a new packet is rejected. The probability of this event is known as BP, which is expressed as

$$P_B = \frac{P_0}{k!}\left(\frac{\gamma}{u}\right)^k \tag{12}$$

IV. Numerical Results and Discussions

Fig. 6 shows the minimum of the labeled bits L versus the stacked label number k for M-sequence and stuffed quadratic congruence (SQC) codes. The parameters for both codes are respectively $(N,\omega,\lambda) = (15,84)$ and $(13,41)$, where the sequences with similar codes lengths are selected for fair comparisons. The difference in the L values between M-sequence and SQC comes from the different noise levels raised in the decoding process. M-sequence label suffers a larger noise variance than the SQC one when decoded due to the lower ratio of ω/λ. It results in a larger L as more labeled bits must be decoded to obtain the desired switch result and reduce the noise effect. Similarly, L values increase with k since a large k also indicates a high noise power.

The parameters used for simulations are $P_{sr} = -20$ dBm, $R = 0.95$ A/W, $B = 10$ GHz, $v = 3.75$ THz, $S_{th} = 1.29 \times 10^{-24}$ W/Hz.

In Fig. 7, L is plotted against the effective power P_{sr} when $\alpha = 10^{-9}$ and $k = 6$ and 12 for M-sequence and SQC codes. L is observed high when P_{sr} is sufficiently small and becomes nearly constant when P_{sr} is relatively large. This characteristic of L variations comes from the dominating noise factors under different signal levels. When the signal power is small, the noise power is mainly contributed by thermal noise, which can be mitigated by simply increasing P_{sr}. However, as the signal power becomes large, the effect of phase-intensity induced noise (PIIN) emerges. Since PIIN variance is positively related to $(P_{sr})^2$, its effect cannot be suppressed even if the power level is high.

Fig. 8 shows that when a required significance level α reduces, L correspondingly increases. In this figure, k and P_{sr} are respectively set to 12 and -20 dBm. A low α indicates a low probability of rejecting H_0, resulting in a higher chance of correct switching. More labeled bits are required to get sufficiently enough results of correct decoding to alleviate the noise effect. Moreover, the SQC labels do not suffer as much noise power as the M-sequence ones, so they have a smaller L, corresponding to the previous figures' characteristics.

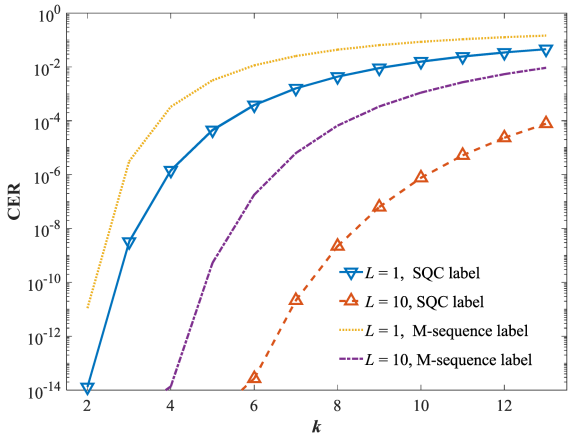

Fig. 9. CER versus k for SQC and M-sequence labels.

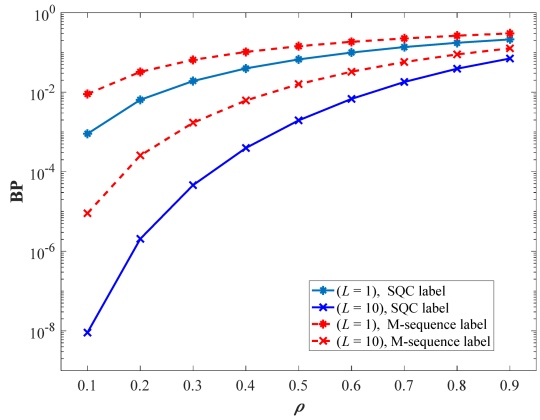

Fig. 10. BP versus traffic intensity for SQC and M-sequence labels.

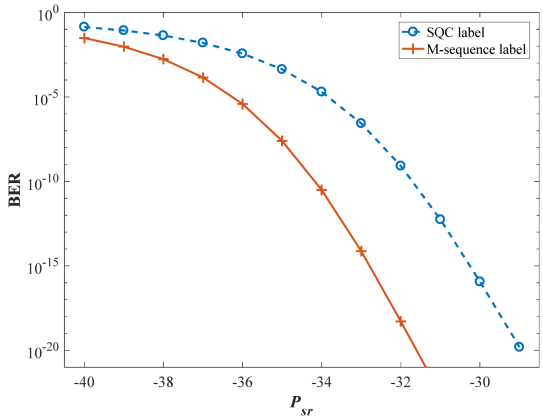

Fig. 11. BER versus Psr for SQC and M-sequence labels.

Finally, based on hypothesis testing, we analyze the code-error rate (CER) of SAC labels with and without the proposed labeling detecting scheme. In the testing, significance level α is defined as the probability of accepting the alternative hypothesis even if the null one is true. According to the hypothesis definitions, α can be seen as CER as it depicts the case that the code-detecting scheme fails to identify the desired label from a stack. Fig. 9 shows that the proposed method reaches lower CER values for both SQC and M-sequence labels, compared with the existing balanced detection of decoding SAC signals [23]–[25].In the previous methods, OCDM labels are decoded individually, which can be seen as a unit labeled-bit case ($L = 1$). The CER improvement results from averaging the decoding results of multiple labeled bits ($L = 10$) in the proposed scheme.

Given the results in Figs. 8 and 9, one could explore how the proposed scheme can be used in multi-service transmission scenarios. As an increased L results in a reduced α or CER, assigning the users of different classes with a different L is a possible solution. A specific CER for a given user class can be reached by encoding a label stack on the required number of payload bits. Since only fixed-weight codes are employed in this paper, the efficiency of multiservice transmissions can be further enhanced by adopting the multi-length variable-weight (MLVW) codes in [26]. By flexibly selecting the combination of the code weight value and the labeled bit number, the network can support diversified levels of QoS. Different error probabilities can be achieved for a given labeled bit number by encoding the payload with labels with various code weights.

Fig. 10 shows BP versus traffic intensity ρ for the packets labeled with SQC and M-sequence codes. Increasing ρ indicates a higher possibility that the available labels are fully distributed, resulting in a higher BP, where ρ is traffic intensity defined as γ/u. In the proposed scheme of label detection, hypothesis testing is employed to retrieve the label information carried by multiple payload bits. Previous analysis has shown that increasing the labeled bit number L reduces the noise effect shown at a decoder and therefore reaches a CER. Therefore, the proposed scheme supports an increased label number k carried by a single packet. For a CER threshold close to 10^{-9}, the carried label numbers of SQC and M-sequence codes are increased from 2 and 3 for $L = 1$ to 5 and 8 for $L = 10$. The BP values for both labels are correspondingly decreased due to the enlarged system capacity.

The BER versus the effective power P_{sr} is plotted in Fig. 11 when the stacked label number $k = 6$. With the increment of P_{sr}, M-sequence code reaches a lower BER than SQC code due to its higher code weight contributing to a larger current mean. Despite the reduced current variance of SQC code suppressed by its low cross-correlation, the lower code weight still results in a small signal-to-noise (SNR) value. Both payloads realize an acceptable BER of 10^{-9} when P_{sr} exceeds -32 dBm. Since the general power value is -20 dBm, the network supports payload detection with good BER performance.

V. Conclusion

This paper presents a novel labeling scheme of inscribing stacked SAC labels in a part of payload bits in OPS networks. The modules of label generation and detection at network nodes have been described. The photocurrent mean of the decoded labeled bits is employed as the index of the switching decision. The number of the encoded payload bits is derived based on hypothesis testing to provide a requested CER. The testing scenario is described as the Gaussian model of the noise characteristics in the decoding process. Numerical results reveal that a larger number of encoded bits is required for noise-dominant

conditions, such as employing high cross-correlation codes or receiving the low-power labels. Reliable label recognition in packet switching can be achieved by analyzing the overall decoding results of the labeled bits instead of considering each labeled signal individually.

REFERENCES

[1] M. Masood, M. M. Fouad, R. Kamal, I. Glesk, and I. U. Khan, "An improved particle swarm algorithm for multi-objectives based optimization in MPLS/GMPLS networks," *IEEE Access*, vol. 7, pp. 137147–137162, 2019, doi: 10.1109/ACCESS.2019.2934946.

[2] M. Kanj, E. L. Rouzic, J. Meuric, and B. Cousin, "Optical power control in translucent flexible optical networks with GMPLS control plane," *J. Opt. Commun. Netw.*, vol. 10, no. 9, pp. 760–772, Sep. 2018, doi: 10.1364/JOCN.10.000760.

[3] A. E. Farghal, H. M. H. Shalaby, and Z. Kawasaki, "Multirate multiservice all-optical code switched GMPLS core network utilizing multicode variable-weight optical code-division multiplexing," *J. Opt. Commun. Netw.*, vol. 6, no. 8, pp. 670–683, Aug. 2014, doi: 10.1364/JOCN.6.000670.

[4] Y. Wang and B. Li, "Optical code-labeled router based on OCDM," *J. Opt. Commun. Netw.*, vol. 2, no. 2, pp. 111–116, Feb. 2010, doi: 10.1364/JOCN.2.000111.

[5] K. S. Chen, "Packet switching strategy and node architecture of extended spectral-amplitude-coding labels in GMPLS networks," *Appl. Sci.*, vol. 9, no. 7, Apr. 2019, Art. no. 1513, doi: 10.3390/app9071513.

[6] C. Chang, G. Yang, I. Glesk, and W. C. Kwong, "On the performance of the effects of temperature variation in ultrafast incoherent fiber-optic CDMA systems with SOA-based tunable dispersion compensator," *IEEE Photon. J.*, vol. 11, no. 3, Jun. 2019, Art. no. 7203110, doi: 10.1109/JPHOT.2019.2917818.

[7] C. Tsai, G. Yang, J. Lin, C. Chang, I. Glesk, and W. C. Kwong, "Pulse-power-detection analysis of incoherent O-CDMA systems under the influence of fiber temperature fluctuations," *J. Lightw. Technol.*, vol. 35, no. 12, pp. 2366–2379, Jun. 2017, doi: 10.1109/JLT.2017.2690992.

[8] A. E. A. Farghal, H. M. H. Shalaby, K. Kato, and R. K. Pokharel, "Performance analysis of multicode OCDM networks supporting elastic transmission with QoS differentiation," *IEEE Trans. Commun.*, vol. 64, no. 2, pp. 741–752, Feb. 2016, doi: 10.1109/TCOMM.2015.2512922.

[9] H. Beyranvand and J. A. Salehi, "Application of optical multilevel transmission technique in WDM/OCDM-based core networks," *IEEE Commun. Mag.*, vol. 52, no. 8, pp. 116–125, Aug. 2014, doi: 10.1109/MCOM.2014.6871679.

[10] A. E. A. Farghal and H. M. H. Shalaby, "Reducing inter-core crosstalk impact via code-interleaving and bipolar 2-PPM for core-multiplexed SAC OCDMA PON," *J. Opt. Commun. Netw.*, vol. 10, no. 1, pp. 35–45, Jan. 2018, doi: 10.1364/JOCN.10.000035.

[11] K. B. Huang, M. Murata, and K. Kitayama, "Variable bandwidth optical paths: Comparison between optical code labelled path and OCDM path," *J. Lightw. Technol.*, vol. 24, no. 10, pp. 563–573, Oct. 2006, doi: 10.1109/JLT.2006.872319.

[12] F. Solano, T. Stidsen, R. Fabregat, and J. L. Marzo, "Label space reduction in MPLS networks: How much can a single stacked label do?," *IEEE/ACM Trans. Netw.*, vol. 16, no. 6, pp. 1308–1320, Dec. 2008, doi: 10.1109/TNET.2007.912382.

[13] K. S. Chen and C. C. Yang, "An application of spectral-amplitude-coding labels in optical signal buffering over optical packet-switching networks," *IEEE Commun. Lett.*, vol. 24, no.no. 9, pp. 2020–2023, Sep. 2020, doi: 10.1109/LCOMM.2020.2997024.

[14] Y. B. M'Sallem, P. Seddighian, L. A. Rusch, and S. LaRochelle, "Optical packet switching via FWM processing of time-stacked weight-2 codes," *IEEE Photon. Technol. Lett.*, vol. 20, no. 20, pp. 1712–1714, Oct. 2008, doi: 10.1109/LPT.2008.2003421.

[15] A. Cherifi, N. Jellali, M. Najjar, S. A. Aljunid, and B. S. Bouazza, "Development of a novel two-dimensional-SWZCC–code for spectral/spatial optical CDMA system," *Opt. Laser Technol.*, vol. 109, pp. 233–240, Jan. 2019, doi: 10.1016/j.optlastec.2018.07.078.

[16] K. S. Nisar, H. Sarangal, and S. S. Thapar, "Performance evaluation of newly constructed NZCC for SAC-OCDMA using direct detection technique," *Photon. Netw. Commun.*, vol. 37, pp. 75–82, Feb. 2019, doi: 10.1007/s11107-018-0794-4.

[17] C. C. Yang, "Hybrid wavelength-division-multiplexing/spectral-amplitude-coding optical CDMA system," *IEEE Photon. Technol. Lett.*, vol. 17, no. 6, pp. 1343–1345, Jun. 2005, doi: 10.1109/LPT.2005.847447.

[18] H. C. Cheng, C. H. Wu, C. C. Yang, and Y. T. Chang, "Wavelength division multiplexing/spectral amplitude coding applications in fiber vibration sensor systems," *IEEE Sensors J.*, vol. 11, no. 10, pp. 2518–2526, Oct. 2011, doi: 10.1109/JSEN.2011.2128308.

[19] K. S. Chen, "Label stacking scenarios in hybrid wavelength and code-switched GMPLS networks," *Electronics*, vol. 7, no. 10, pp. 251, Oct. 2018, doi: 10.3390/electronics7100251.

[20] J. R. de Almeida Amazonas, G. Santos-Boada, and J. Solé-Pareta, "Who shot optical packet switching?," in *Proc. 19th Int. Conf. Transp. Opt. Netw.*, Girona, Spain, 2017, pp. 1–4, doi: 10.1109/ICTON.2017.8025164.

[21] C. C. Yang, "Compact optical CDMA passive optical network with differentiated services," *IEEE Trans. Commun.*, vol. 57, no. 8, pp. 2402–2409, Aug. 2009, doi: 10.1109/TCOMM.2009.08.070519.

[22] J. Sztrik, *Basic Queueing Theory: Foundations of System Performance Modeling*. Saarbrücken, Germany: GlobeEdit, 2016.

[23] K. S. Nisar, "Numerical construction of generalized matrix partitioning code for spectral amplitude coding optical CDMA systems," *Optik*, vol. 130, pp. 619–632, Nov. 2017, doi: 10.1016/j.ijleo.2016.10.110.

[24] C. C. Yang, J. F. Huang, H. H. Chang, and K. S. Chen, "Radio transmissions over residue-stuffed-QC-coded optical CDMA network," *IEEE Commun. Lett.*, vol. 18, no. 2, pp. 329–331, Feb. 2014, doi: 10.1109/LCOMM.2013.120613.131527.

[25] C. T. Yen, J. F. Huang, and W. Z. Zhang, "Hiding stealth optical CDMA signals in public BPSK channels for optical wireless communication," *Appl. Sci.*, vol. 8, no. 10, Sep. 2018, Art. no. 1731, doi: 10.3390/app8101731.

[26] H. Beyranvand, S. A. Nezamalhosseini, J. A. Salehi, and F. Marvasti, "Performance analysis of equal-energy two-level OCDMA system using generalized optical orthogonal codes," *J. Lightw. Technol.*, vol. 31, no. 10, pp. 1573–1584, May 2013, doi: 10.1109/JLT.2013.2250914.